

SANDIA REPORT

SAND2009-44534453

Unlimited Release

Printed July 2009

Prepared November 2004

Feasibility of Nuclear Sensing for Horizontal Directional Drilling

Nathan R. Hilton, Doug Archer, Jim Brennan, John Estrada, Jim Lund, and Allen Salmi

Prepared by
Sandia National Laboratories
Albuquerque, New Mexico 87185 and Livermore, California 94550

Sandia is a multiprogram laboratory operated by Sandia Corporation,
a Lockheed Martin Company, for the United States Department of Energy's
National Nuclear Security Administration under Contract DE-AC04-94AL85000.

Approved for public release; further dissemination unlimited.

Issued by Sandia National Laboratories, operated for the United States Department of Energy by Sandia Corporation.

NOTICE: This report was prepared as an account of work sponsored by an agency of the United States Government. Neither the United States Government, nor any agency thereof, nor any of their employees, nor any of their contractors, subcontractors, or their employees, make any warranty, express or implied, or assume any legal liability or responsibility for the accuracy, completeness, or usefulness of any information, apparatus, product, or process disclosed, or represent that its use would not infringe privately owned rights. Reference herein to any specific commercial product, process, or service by trade name, trademark, manufacturer, or otherwise, does not necessarily constitute or imply its endorsement, recommendation, or favoring by the United States Government, any agency thereof, or any of their contractors or subcontractors. The views and opinions expressed herein do not necessarily state or reflect those of the United States Government, any agency thereof, or any of their contractors.

Printed in the United States of America. This report has been reproduced directly from the best available copy.

Available to DOE and DOE contractors from
U.S. Department of Energy
Office of Scientific and Technical Information
P.O. Box 62
Oak Ridge, TN 37831

Telephone: (865) 576-8401
Facsimile: (865) 576-5728
E-Mail: reports@adonis.osti.gov
Online ordering: <http://www.osti.gov/bridge>

Available to the public from
U.S. Department of Commerce
National Technical Information Service
5285 Port Royal Rd.
Springfield, VA 22161

Telephone: (800) 553-6847
Facsimile: (703) 605-6900
E-Mail: orders@ntis.fedworld.gov
Online order: <http://www.ntis.gov/help/ordermethods.asp?loc=7-4-0#online>



Executive Summary

The goal of this project was to determine the feasibility of finding underground objects using ionizing radiation. In particular, the Sponsor wanted Sandia National Laboratories (SNL) to determine if neutrons or gamma rays could be used as an effective probe to ascertain the presence of underground objects (e.g., conduit, pipe, etc.) forward of an underground boring tool. Further, if the basic feasibility of the method was established, the Sponsor wanted to see how quickly and how far in front of the boring tool the technique was useful.

The form factor requested by the Sponsor was a forward-looking (FL) capability from either a nominal 3.5-inch or 10-inch horizontal, directionally drilled borehole. The borehole would most likely be located in an urban environment. Urban environments are typically high-noise, multiple-source, heterogeneous environments. The resolution of underground objects of interest from clutter (both real and nuisance signals) is especially problematic.

The need for FL technology is a universal ambition for the petroleum, mining, construction, geotechnical engineering, environmental remediation, and utility industries. Drilling hardware configurations, user needs, and sensor physics have combined to produce existing, commercially available nuclear-sensor systems of only a radial, or side-looking (SL), variety. Commercial SL sensors are commonly deployed in vertical boreholes and generally provide only data of large-scale features of the geologic media in subsurface environments. This project is to examine the status quo.

The SNL team considered the following source / detector combinations:

1. gamma source / gamma detector
2. neutron source / gamma detector
3. neutron source / neutron detector

The latter two primarily used continuous fission-spectrum neutron sources, but work with a pulsed fast-neutron source was also begun.

SNL used both a theoretical and an experimental approach to investigate the feasibility of this technique. The theoretical method consisted of computing the transport of neutrons and gamma rays from a source, through soil, and to a detector in order to determine the difference, if any, in the return signal when an object is and is not present. These calculations were usually performed with a modern, three-dimensional radiation transport code, but “paper and pencil” analytical techniques were also employed.

SNL's experimental investigation of the feasibility of the technique consisted of excavating a series of trenches in native soils at the SNL site. In these trenches, SNL placed polyvinyl chloride (PVC) and steel pipe, 3.5 inches in diameter—objects likely to be encountered in an underground urban environment. Mock boreholes, 10 inches in diameter, were constructed perpendicular to the PVC and steel pipe. Into the boreholes were lowered various instrumentation packages containing sources and detectors of ionizing radiation.

Some of the experiments clearly indicated the ability of ionizing radiation to detect buried objects. These experimental results were also corroborated by computer simulations. In particular, SNL found that using a neutron source and a gamma-ray detector to measure the return signal, underground objects could be discerned several inches deep in soil. While the neutron source was found to be an effective probe, the

gamma-ray source was not very useful in discerning objects. In addition, two techniques that looked promising in theory, neutron-neutron and fast neutron, were not conclusively investigated due to technical problems and resource constraints.

Background

Before discussing project specifics, it is first worth reviewing a few general technical concepts that are germane to understanding the work described in this report. This section includes brief definitions and descriptions of the ionizing radiation used as probing agents in our studies, a discussion of radiation transport through matter, and a discussion of how ionizing radiation is detected. We conclude this section with an overview of the work that was performed in this project and a guide to the organization of this report.

Ionizing Radiation

The work described in this report is restricted to investigations utilizing ionizing radiation. These types of radiation, as their name implies, are energetic enough to cause direct ionization of atoms and molecules. By contrast, non-ionizing radiation (such as microwaves or visible light) is of lower energy per quanta and imparts energy via thermal excitation to the material with which it interacts.

There are two general classes of ionizing radiation—neutral and charged particles. Common examples of charged-particle radiation are energetic electrons (beta particles), protons, and alpha particles (helium nuclei). Because charged particles continuously lose energy in matter via electromagnetic interactions, the propagation range in most materials of readily produced charged particles is quite short. With such limited ranges in soil, one can eliminate from consideration the use of most charged particles for the application of discerning underground objects. One important exception are cosmic-ray generated muons, which have such high energies that they can penetrate large thicknesses of rock. However, further discussion of the use of muons is not within the scope of this report.

Neutral particles are the other class of ionizing radiation and are the most applicable for this investigation. The two relevant types of neutral particles are neutrons and energetic gamma rays (photons). Because neutral particles do not continuously lose energy as they pass through matter, their range can be quite long.

Common neutron sources for this application either use natural radioactive emissions or are driven by a small particle accelerator. An example of the former source type, often called radioisotopic, are materials that fission spontaneously, such as californium, or that combine a light element, such as lithium and beryllium, with a radioactive element that emits alpha particles, such as polonium or americium. The alpha particle interacts with the beryllium or lithium and produces a neutron. Common accelerator-based neutron sources accelerate deuterium nuclei into a target containing deuterium or tritium, and the resulting fusion reactions produce fast neutrons. An advantage of most radioisotopic neutron sources is that once they are manufactured they function without any external input. However, because there is no way to stop these sources from producing neutrons, they suffer the corresponding disadvantage of making them much more difficult to transport or deploy. Being a potential homeland security threat, these sources must also be protected from theft and misuse. Accelerator neutron

sources are thus recommended for this application because these neutron sources can be turned off when desired.

Radiation Transport

The passage of ionizing radiation through matter can be quite difficult to calculate quantitatively. Unlike macroscopic particles such as bullets or low-energy microscopic particles like visible light, ionizing radiation can interact with matter via a variety of mechanisms (e.g., scattering and absorption), and these interaction mechanisms are strongly energy and material dependant. Furthermore, when one type of ionizing radiation interacts with matter, additional ionizing radiation (e.g., gamma rays) is often created, which may be of a different type. This new radiation must then also be tracked to quantitatively understand the transport of the ionizing radiation through the material. Physicists and nuclear engineers have vigorously investigated the problem of radiation transport calculations. Computer programs called “transport codes” have been developed during the past fifty years that very accurately simulate complex ionizing radiation interactions in any material. The disadvantage of some transport codes is that they can be tedious to initialize (i.e., specify boundary values for the problem to be analyzed), and they can be slow to execute even on the most powerful computers. Typically, when analyzing a complex problem, crude estimates using analytic approximations are used first to bound the problem and search for promising conditions. After these “back of the envelope” calculations are performed and promising situations identified, the computer transport codes are then applied to a limited series of promising situations. This method of approximate estimate, followed by detailed computer calculation, was the technique SNL used during this project to quantify radiation transport through the soil.

Detection of Ionizing Radiation

Another technical issue, with which the Sponsor must be familiar to understand the substance of this report, is the limitation of radiation detectors. Generally, the problem SNL investigated during this project was the emission of ionizing radiation from a source; the transport of that radiation through the surrounding soil and other materials, which may include an obstacle to detect; and the capture or counting of the ionizing radiation that returns to the detector. If there were perfect radiation detectors, one could simply use transport calculations to understand exactly what types of underground objects one could identify and at what distance. Unfortunately, existing radiation detectors are not perfect. They can be severely limited both in terms of efficiency (i.e., the ability to sense the arriving radiation) and energy resolution (i.e., the ability to discern the exact energy of the detected radiation).

The two types of radiation that SNL detected for this project were neutrons and gamma rays. Without going into the details of how these two types of radiation are detected, we will simply state the limitations of detectors used to detect these two types of radiation. Neutron detectors, in the neutron energy range of interest in this project, are not capable of discerning the energy of neutrons that interact with them (i.e., they have no energy resolution). Although sensitive almost exclusively to thermal neutrons, these detectors simply count the number of all detected neutrons, regardless of their energy. Furthermore, neutron detectors can be quite inefficient. At the neutron energies most useful for this project, it is difficult to obtain detectors with efficiencies greater than a few

percent. In other words, most of the neutrons impinging on the detector pass through the detector without interacting.

The situation for gamma-rays is somewhat better. Methods have been developed to measure the energies of gamma rays that interact with a modern detector; however, there are some trade-offs. One can use cryogenically cooled devices called high-purity germanium (HPGe) detectors to get very good gamma-ray energy resolution, but cryogenic cooling can be awkward and bulky to deploy in the field. Another type of gamma-ray detector that functions at room temperature is called a scintillation detector. While much easier to configure and deploy than HPGe detectors, scintillation detectors have much worse energy resolution.

Overview of activities

This project employed both an experimental and theoretical approach. The theoretical activities involved first estimating, and then computing more precisely using transport codes, the radiation signals expected when an ionizing radiation travels from a source to a buried object and then back to a detector. In the experiments, return signals consist of scattered and unscattered radiation from the primary source, secondary radiation stimulated in the nearby materials, and background radiation from these materials and cosmic sources. However, no background radiation was used in the theoretical calculations, as this background is expected to be both relatively small and equivalent in all cases. Concurrent with these calculations, experiments were performed to see if underground objects could actually be detected using commercially available radiation sources and detectors. These were performed under fairly realistic conditions—underground, out of doors, and using probable target objects and materials.

Obstacle Detection Experiments

Objective of Experiments

The first objective of the obstacle detection experiments was to determine the feasibility of detecting typical underground objects in a 10-inch borehole forward of the drilling apparatus or bit. SNL wished to physically simulate a horizontal underground borehole in relatively dry soil (i.e., above the static water table) and to use commonly encountered objects such as PVC and steel pipe. A second objective of the experiments was to validate the accuracy of the computer simulations.

Description of Experiments

The initial desire in the early phase of the project was to construct an experiment in a horizontal borehole. However, a horizontal experiment was beyond the limited resources of the project. Instead, SNL elected to use a vertical borehole configuration shown in Figure 1 that retained the fidelity necessary to determine the feasibility of the object-detection technique.

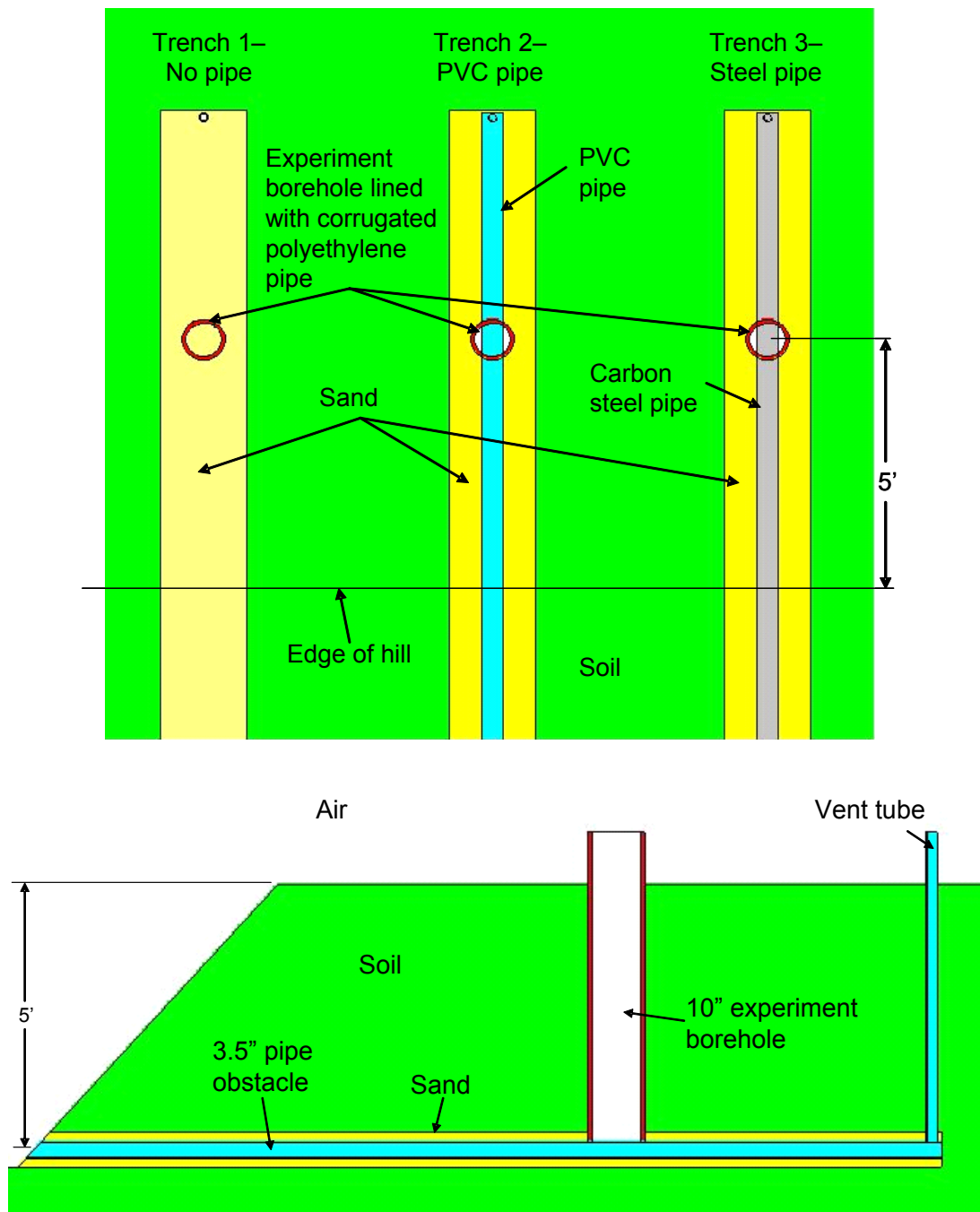


Fig. 1 Diagrams of the SNL test site for the pipe detection experiments. The top view shows three trenches dug into the side of a hill where a steel and PVC pipe were buried horizontally, as best seen in the side view (bottom), in sand with a vertical fill pipe to facilitate filling and emptying it of water.

Obstacle Detection Computer Simulations

Objective of Simulations

Radiation transport and detection computer simulations are useful for investigating situations where physical experiments are not possible for reasons of safety, environmental protection, cost, or time. Because of these advantages, simulations can also provide insight of physical principles that may not be readily discerned from experiments. For example, simulations can remove or mitigate the effects of counting statistics and poor detector responses, which might obscure a signal from a nearby underground object. Once that signal is revealed in such a simulation, it may be more easily recognized in an experiment.

SNL began with simple simulations intended to guide more detailed simulations and, eventually, the design of the physical experiments. Once these experiments were designed and constructed, detailed simulations were then performed. Combined analysis of the experimental and simulation data provides greater confidence in all the simulations and complementary information that aids in understanding the experimental results and in drawing conclusions about how obstacle-detection systems based on radiation interrogation may perform.

Description of Simulations

All radiation transport simulations were performed using MCNP, which is a Monte Carlo radiation transport code developed and maintained by Los Alamos National Laboratory. This commonly used software has been extensively tested and benchmarked with physical experiments. Only a portion of the simulation results are presented hereafter, and these simulations are for the geometries shown in Figure 2, which closely match the experimental geometries. Not shown in Figure 2 are the dimensions of and among the various components. An important dimension is the depth of the sand covering the pipe, which was 2 inches in all simulations. Secondly, a stand-off of 1 inch existed between the top of the sand and both the source and the front (i.e., lowest) surface of the detector. Lastly, in separate simulations the source and detector were arranged either parallel or perpendicular to each object, as shown in Figure 2. Because the source and detector are not rotationally symmetric about the borehole axis it was necessary to test both parallel and perpendicular object orientations. The simulated radiation sources were either ^{137}Cs , which primarily emits 662-keV gamma rays, or ^{252}Cf , which emits fission neutrons with an average energy of 2.35 MeV as well as gamma and X rays with numerous energies. The photon emissions of the ^{252}Cf source were not included in these simulations. Hereafter, the ^{137}Cs and ^{252}Cf sources are referred to simply as photon and neutron sources, respectively.

In analogy with the detectors used in the experiments, the simulated photon detector is a 2-inch diameter, 2-inch long sodium iodide (NaI) crystal, and the neutron detector is a 2-inch diameter, 9.75-inch long tube of ^3He gas at a pressure of 4 atmospheres. The energy-dependent interaction rates correspond to these simulated detector volumes. Computer simulations have an advantage that allows discernment of physical effects that may otherwise be too subtle to be noticed in some physical experiments. The simulations performed for this project computed spectra of photon energy deposition in the NaI detector without folding in energy-dependent detector

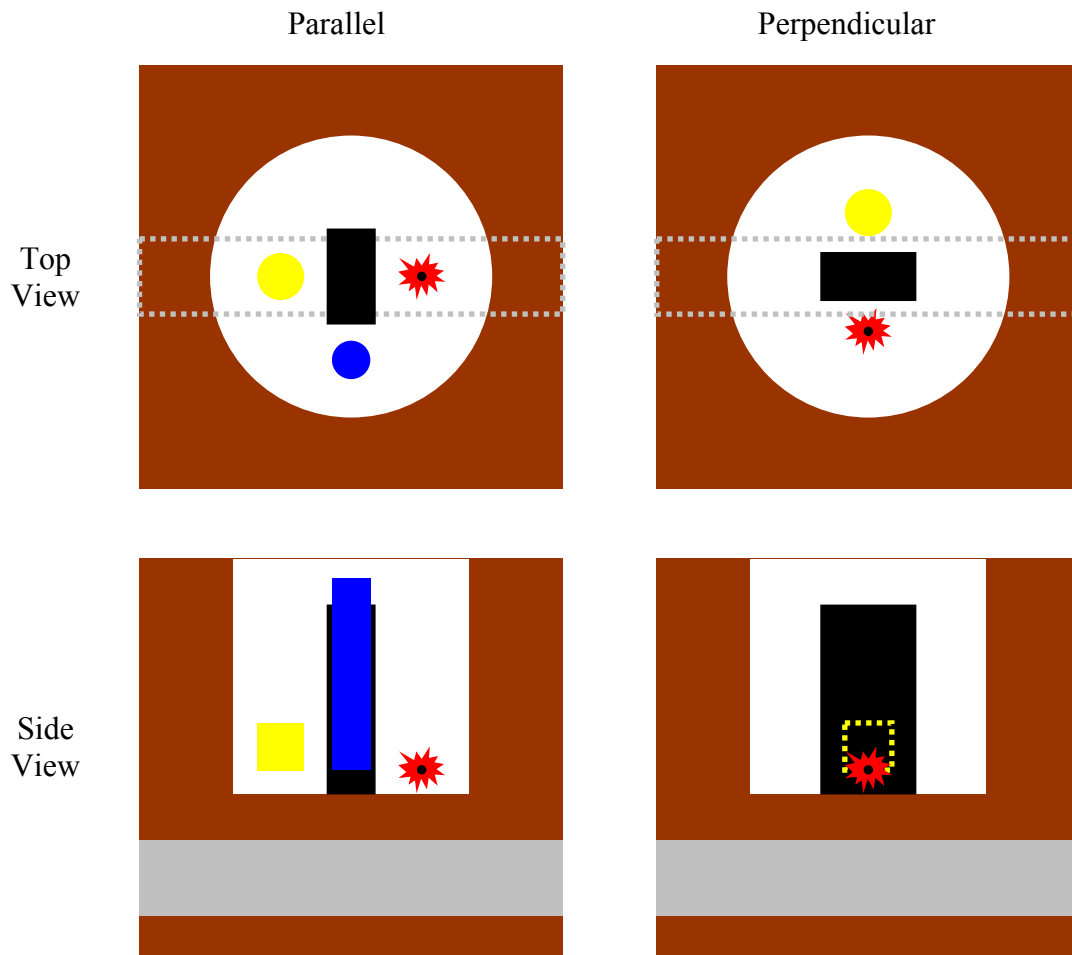


Fig. 2 Illustration showing the arrangements of the gamma or neutron source (red), gamma detector (yellow), neutron detector (blue), lead shield (black), pipe (grey), and surrounding soil/sand (brown) for both the experiments and simulations. The neutron detector was not used with the gamma source, and only the configuration shown was used with the neutron source. Sand 2 to 4 inches deep covered and surrounded each pipe, and native soil was used elsewhere.

response characteristics dealing with how that deposited energy is converted into a signal and measured. Signal generation and measurement are affected by random processes (and systematic biases) that impart uncertainty (and error) to the measurement of the signal. Specifically, these computed spectra include only those parts of the detector response function that affect how much energy an incident photon deposits in the detector (e.g., escape of photoelectric-absorption X rays, Compton scattering). All other factors of the detector response function are excluded (e.g., stochastic and nonlinear scintillation-light production, inhomogeneous light collection, and noisy readout electronics). Thus, these photon simulation data are qualitatively different from corresponding experimental data, which include effects of the complete detector response function.

Separate simulations were performed with and without each object present using: (1) the photon source with the photon detector or (2) the neutron source with both the

neutron and photon detectors simultaneously. The simulations and experiments of the first case are referred to hereafter as the photon/photon method. Likewise, those of the second case are described as either the neutron/neutron or neutron/photon methods.

Results and Analysis

Photon/Photon Method

Figure 3 shows the results of two photon/photon simulations of an air-filled steel-pipe obstacle. This figure plots the calculated, unnormalized probability distribution of photon energy deposited in the NaI detector. Due to the nature of Monte Carlo calculations and finite computer resources, uncertainty in the estimated values of the probability distribution is apparent from the jaggedness of the curves, primarily for energy bins where the probabilities are lowest. Analysis of these data reveals that there is no statistically significant difference between the signals one would expect to measure with the pipe oriented either parallel or perpendicular to source/detector assembly. However, the experimental data do show small differences, which reinforce the concept that there are often variations in physical experiments that likely cannot be known and/or compensated for in the data analysis.

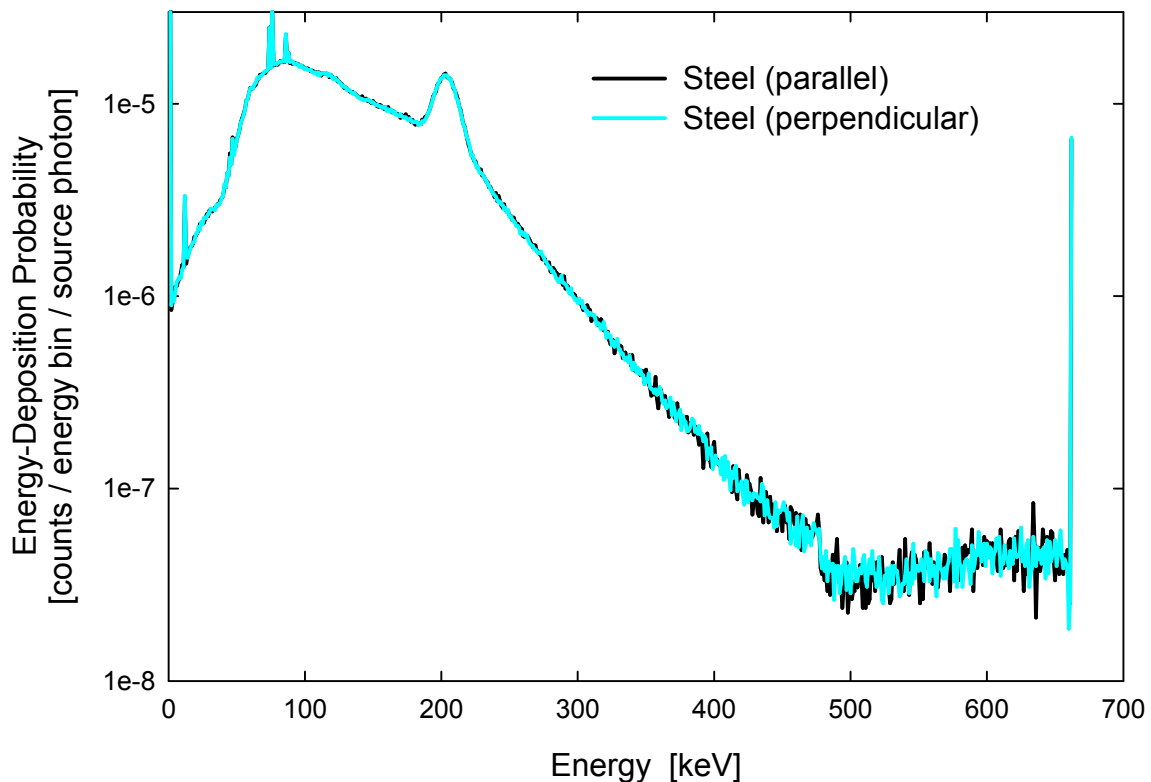


Fig. 3 Photon/photon simulation of steel pipe obstacle at 2 inch depth that is either parallel or perpendicular to the source/detector assembly.

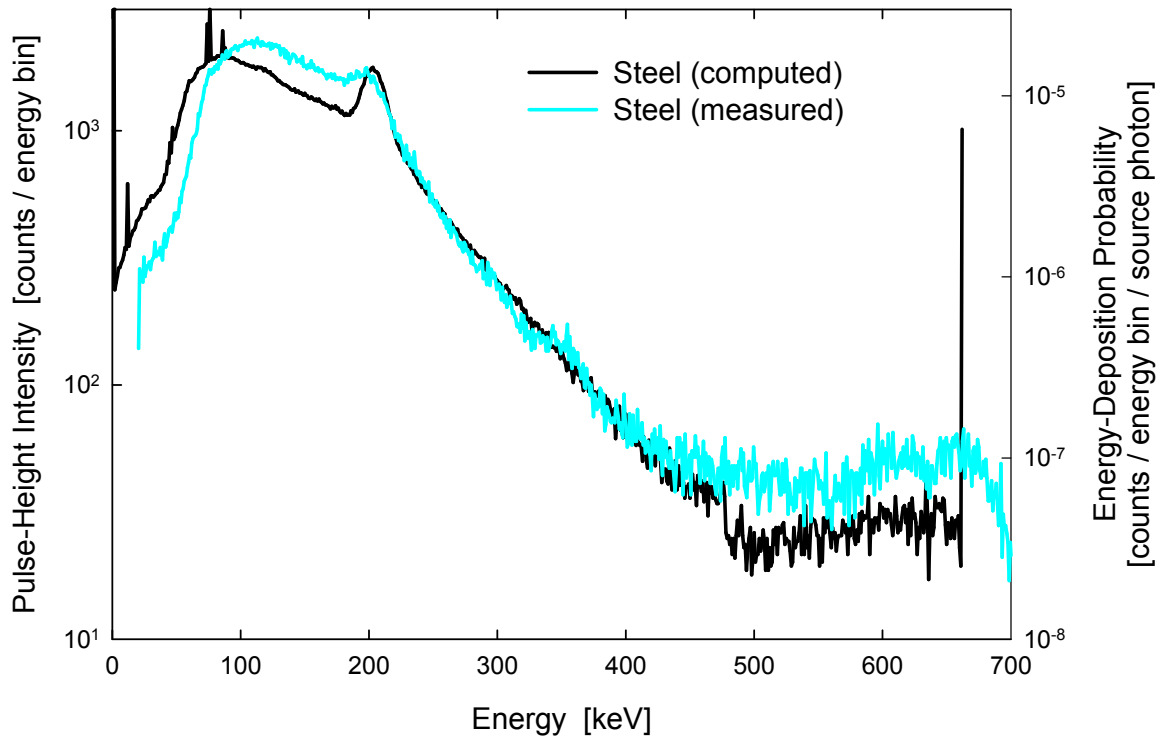


Fig. 4 Photon/photon simulation and experiment with a steel pipe at approximately a 2 inch depth that is parallel to the source/detector assembly.

In other words, these simulations lack the random irregularities in the native soil, sand, pipes, radiation source, etc. that are important enough to noticeably affect real measurements. Nevertheless, these simulations contain real features that provide useful information. Figure 4 shows the reasonable agreement anticipated between the simulation and experimental data. Examination of the simulation data may indicate what types of objects may be detected at what distances using a given technique (e.g., photon/photon, neutron/photon, or neutron/neutron). Doing so in a real experiment, however, is hampered by all of the unknown irregularities in the experiment.

Figure 5 shows results of additional photon/photon simulations. At the top of Figure 5, the calculated energy-deposition spectra with and without each pipe object shows that certain objects should produce scattered photon signals that are noticeably different from those produced either by other objects or the absence of an object. The spectral peak at just above 200 keV is where one expects to see numerous photons that have undergone a single Compton-scattering event in the surrounding materials before entering the detector. This peak corresponds to a scattering angle of about 140 degrees, which is consistent with expectations for this geometry of source, shield/collimator, and detector. The sharp peaks between 70 and 90 keV are fluorescence X rays from the lead brick, which shields the detector from direct illumination of the source. The broad peak spanning roughly from 50 to 175 keV is due to photons that have undergone multiple scattering events. Details of the effects a particular underground object should have on the photon spectra can be better seen and quantified by taking the difference between energy-deposition spectra with and without an object present. Plotted at the bottom of Figure 5 are the spectra without an object present subtracted from spectra with each

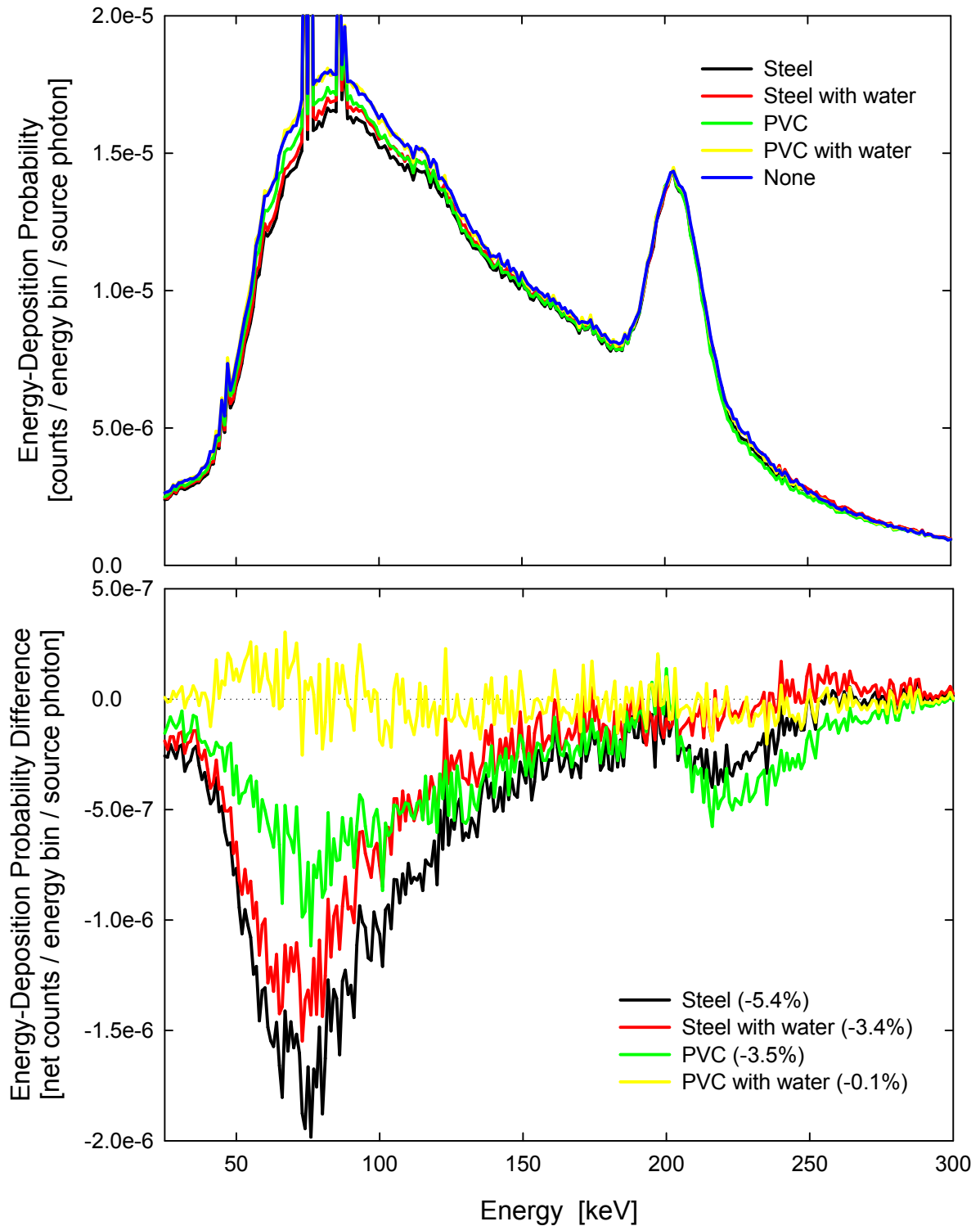


Fig. 5 Photon/photon simulations with and without each pipe obstacle (top). Data without an obstacle subtracted from data with each obstacle (bottom); the integrated difference in percent is shown in the legend within parentheses for each obstacle. All obstacles are at 2 inch depths and parallel to the source/detector assembly.

object. Perhaps the most promising analysis of the difference signals plotted in Figure 5 is the integral of all differences between 25 and 300 keV. Relative to the integrated signal without an object, the empty steel pipe is seen to produce a 5.4% reduction in the scattered photon intensity. Data for the other three objects are also shown.

In photon-backscatter imaging, low-atomic-number objects appear brighter (i.e., more photons scattered by the object successfully return to the detector) than either voids or high-atomic-number objects. Voids allow the interrogating photons to pass further from the detector so any subsequently scattered photons are less likely to return to the detector. High-atomic-number materials absorb more of the scattered photons. Although increasing the energy of incident photons from 662 keV would allow greater penetration into the soil, backscattered (i.e., ~180-degree scattered) photons would always have energies below 256 keV, which makes the range of depths for which this method is sensitive essentially unchanged by increasing the incident photon energy. Thus, in terms of percent difference, the polarity of the difference signal for the steel pipe and the relative order of signals for all the objects were mostly expected, although the relative ordering of the PVC and water-filled steel pipe was not predictable. These two cases are both combinations of backscatter signal enhancers and degraders whose net effects were not predictable but were expected to yield fewer scattered photons than the PVC pipe with water. Simulations of the latter showed that it produces a change so slight to the radiation reaching the detector that it is practically indistinguishable from the case with no object present.

Although differences in these computed energy-deposition spectra are relatively small, one would expect to find a similar difference in pulse-height spectra (i.e., histograms of the amplitudes of detector pulses) from corresponding experimental measurements. However, this differencing analysis of the experimental data acquired, which are shown in Figure 6, does not yield an experimental result consistent with these expectations. Experimental data acquired using the same source/detector assembly configuration as in the simulations is presented in the top graph of Figure 6. In each experiment, photon pulse-height histograms were collected for a detector live time of 600 seconds, and the measured spectra without an object present were subtracted from spectra with each object. Histograms of net counts are plotted versus photon energy based on calibrations using ^{137}Cs and ^{133}Ba sources. While the measured data with the water-filled PVC pipe may be consistent with the simulations, data from the other three pipes are not consistent. Furthermore, experimental measurements with the source/detector assembly rotated perpendicular to the pipes yielded data that is qualitatively and quantitatively distinct from both measurement and simulation results in the parallel orientation. Unfortunately, the radial offsets of the source and detector impart significant orientation-dependent variability to the photon/photon signals of objects that do not have rotationally symmetric shapes or are located off-axis. A system designed with the source, collimator, and detector in a concentric cylindrical arrangement may mitigate this variability as well as focus more of the system's object sensitivity to the volume directly in the path of the boring tool. However, the overall sensitivity of such a design would be greatly restricted in order to fit into a 3.5-inch diameter borehole.

One can draw the following conclusions from these photon/photon data. Although effects that are present in simulations are usually also noticeable in an experiment, additional variability in experiments can perturb, or even mask, these effects.

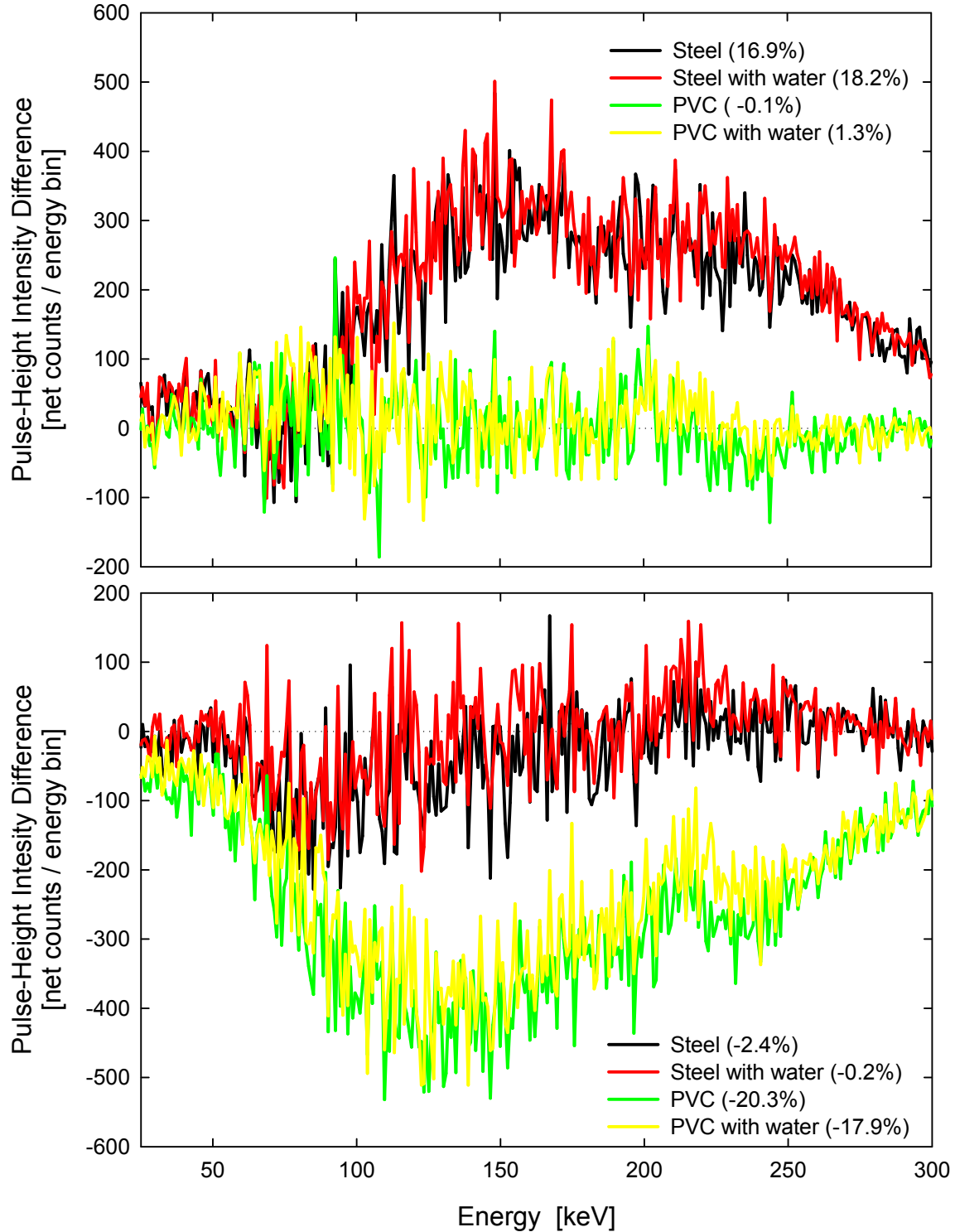


Fig. 6 Photon/photon measurements with and without a pipe obstacle that is or is not filled with water. Data without an obstacle is subtracted from data with each obstacle and plotted for scenarios where the obstacle is parallel (top) and perpendicular (bottom) to the source/detector assembly. The integrated difference in percent is shown in the legend within parentheses for each obstacle. All obstacles are approximately at 2 inch depths.

The implications of these results for using the photon/photon method to detect objects in underground environment are: (1) some objects may go undetected and (2) when an object is detected, determining whether that object is benign clutter or an object of interest is unlikely.

Neutron/Photon Method

Together with the experiments using neutron sources to interrogate the area of interest, SNL performed corresponding neutron-source simulations. Figure 7 presents some of the simulation data for a ^{252}Cf neutron source creating photons in the surrounding materials that are subsequently detected. The neutron energy spectrum from this spontaneously fissioning source induces gamma-ray emissions through both inelastic scattering of fast neutrons as well as capture of slower neutrons. These induced photons have characteristic, discrete energies for each isotope that interacts with the incident neutrons. Some of these discrete-energy photons scatter in the surrounding materials and/or the detector, which results in a broad, continuous distribution of photon energy deposition in the detector that is superposed with numerous discrete photopeaks. In other words, the peaks with relatively high probabilities seen in these spectra result from characteristic photon emissions rather than the statistical “noise” inherent in a Monte Carlo radiation transport calculation. Events in which less than 1 MeV was deposited were tallied into narrower energy bins than those above 1 MeV (i.e., 2 keV versus 10 keV), which allows more closely spaced photopeaks to be discerned below 1 MeV but which increases the relative uncertainty of calculated photon energy deposition in that energy range.

Integrating these spectra across a broad energy range of 0 to 7 MeV sums most of the detected characteristic photons (both scattered and unscattered) induced by the neutron interrogation. Applying the same differencing method used to analyze the photon/photon data yields the percentages listed in the legend of Figure 7, which are the percentage change of the energy-deposition probability (i.e., the number of times per source neutron in which a given energy is deposited in the detector) integrated from 0 to 7 MeV with each object relative to the case with no object present. Because of this large integration range, the simulation was able to converge very well and yield percentage differences P with an estimated relative accuracy of (σ_p/P) ; ± 0.004 .

As expected, when a pipe without water is present the number of induced photons arriving at the detector is reduced because the empty pipe behaves as a void. Neutrons readily travel through the air inside the pipe to the opposite side where any induced photons, or indeed scattered neutrons, are now farther away from the neutron and photon detectors that might see them. In fact, the lower density of PVC compared to steel makes the empty PVC pipe more void-like and causes a correspondingly larger reduction in the returning photon signal. A similar relative reduction is also seen with the PVC and steel pipes that are filled with water. The addition of water to each pipe increases their densities (specifically the densities of induced-photon emitting isotopes) such that in both cases more photons are created that return to the detector than do from either native soil or empty pipes. Unfortunately, the combination of opposing effects implies that both PVC and steel pipes could be partially filled with just enough water to cause these effects to exactly cancel each other over this range of integration.

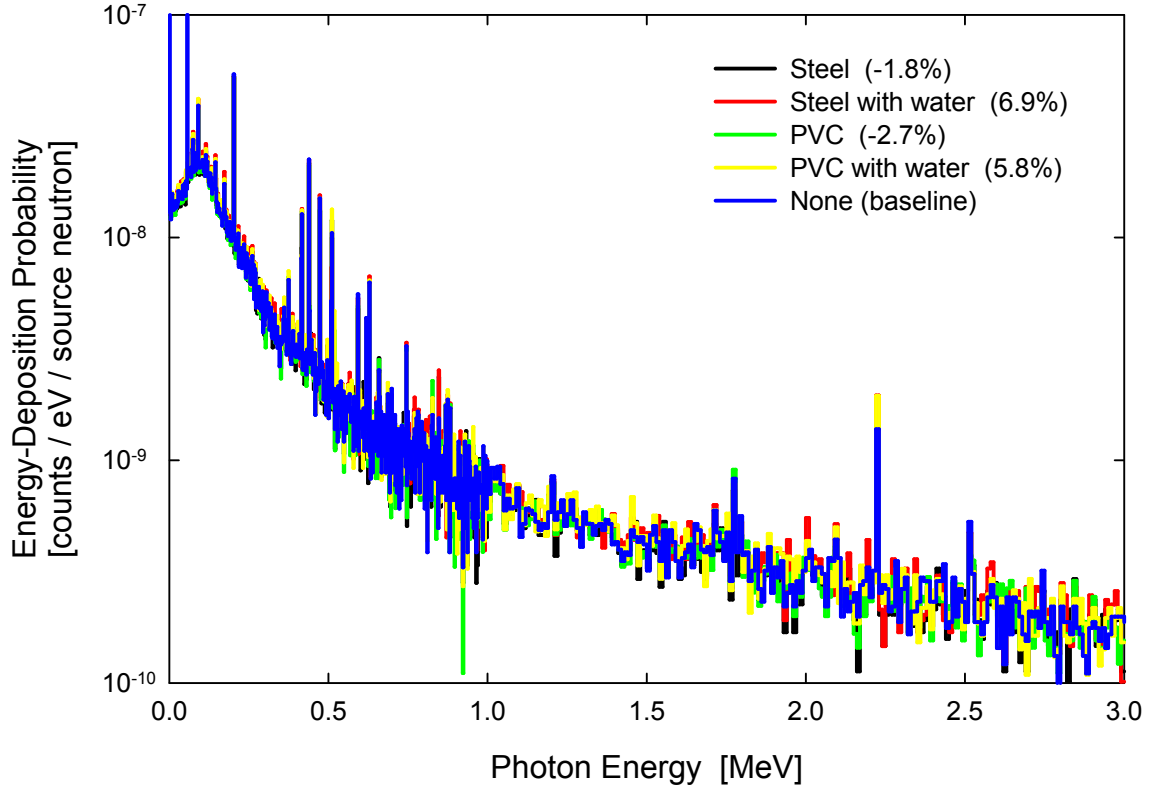


Fig. 7 Neutron/photon simulations with and without each pipe obstacle. All obstacles are at 2 inch depths and parallel to the source/detector assembly. Either 2 or 10 keV bins used below or above 1 MeV, respectively. The relative energy-deposition probability differences integrated from 0 to 7 MeV are shown in parentheses in the legend for each obstacle.

The data in Figure 8 are the same neutron/photon simulation data used in Figure 7 plotted instead as the signal differences. The effects of taking the difference of two stochastically computed numbers is clearly evident, especially below 1 MeV where the energy bins were smaller, and motivates use of an analysis method that mitigates these effects by integrating many such values. The relative difference percentages reported in Figure 7 integrate an energy span from 0 to 7 MeV. Nevertheless, an important characteristic photon emission is the 2.223 MeV photon resulting from fusion of an incident neutron with a proton, which are abundant in water. By integrating only a narrow energy band to include this emission, the relative signals show very strongly the presence of water. It should be noted that because of the small range of integration of these simulation data, the percentages shown in Figure 8 have a relative accuracy of only (σ_p/P) ; ± 0.12 . Performing a longer Monte Carlo simulation would improve these estimates, but clearly the presence of such quantities of water in each pipe should be easily detected if a photon detector with sufficient detection efficiency and energy resolution were used. However, soil and other materials may also have a certain amount of water present that could be displaced by a pipe with an equivalent amount of water. Such an object would also not be seen using an analysis with this range of integration.

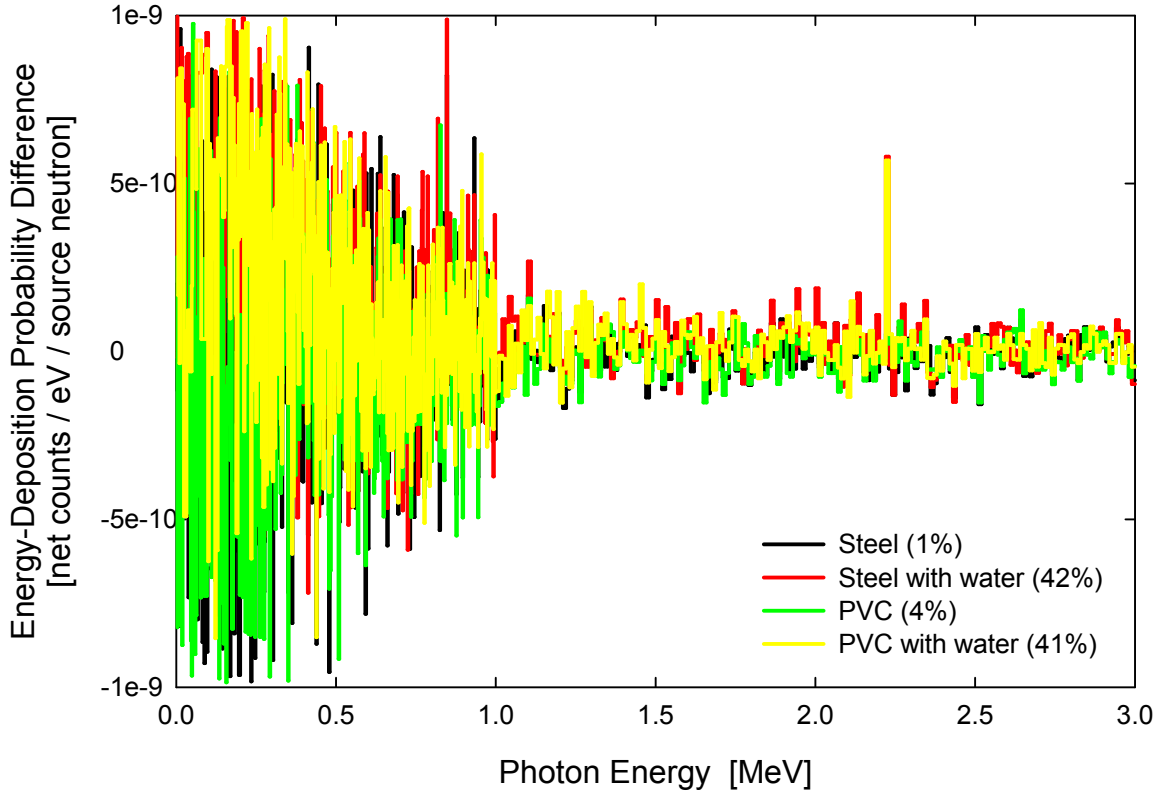


Fig. 8 The same neutron/photon simulation data plotted in Figure 7 shown here as signal differences with and without each pipe obstacle at 2 inch depths and parallel to the source/detector assembly. Either 2 or 10 keV bins used below or above 1 MeV, respectively. The relative integrated differences shown in parentheses in the legend are for data integrated only from 2.22 to 2.23 MeV, which includes the 2.223 MeV photon emitted with neutron capture by hydrogen.

Thus, detector inadequacies combined with numerous other variations (e.g., moisture and other elemental concentration and distribution variations of nearby materials that strongly affect the induced-photon emissions and detection likelihood) that are present in real experiments produce data that is not always consistent with expectations drawn from computer simulations. Figures 9 and 10 present results of neutron/photon experiments where the objects were covered with 4 inches of sand. A ^{252}Cf source was used, which was shielded from a 2-inch NaI detector by a 2-inch thick lead brick. Pulse-height spectra were acquired with the NaI detector for a detector live time of 600 seconds. Differences between spectra with and without each object are shown in Figure 9. As with the photon/photon data, the first observation one can make from these neutron/photon data is that the orientation of the source/detector assembly affects both the relative and absolute signal strengths from these objects. Nevertheless, the second observation from Figure 9 is that all of these particular objects appear to be detectable at a distance of 4 inches.

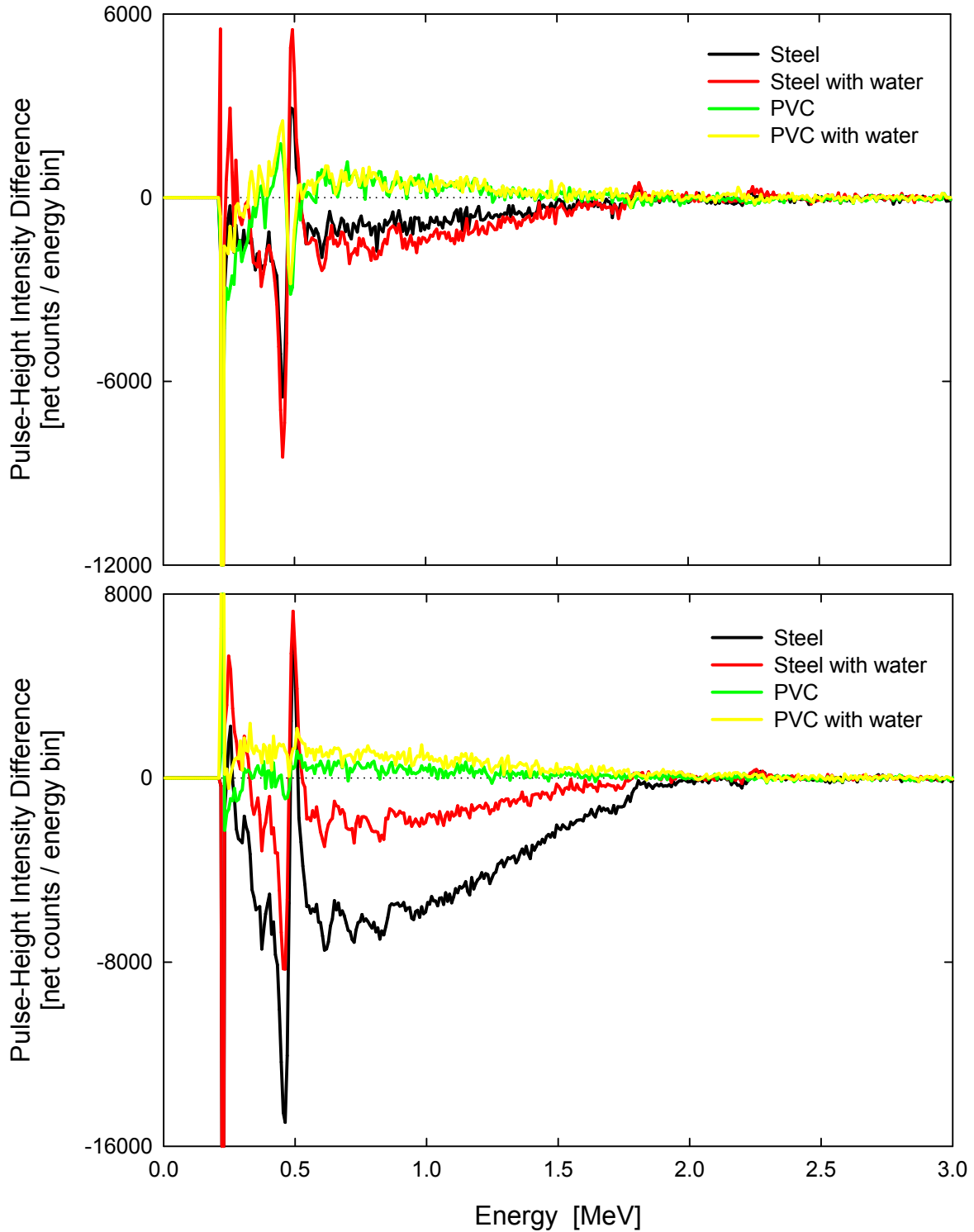


Fig. 9 Measured neutron/photon relative signal differences with and without each pipe obstacle parallel (top) or perpendicular (bottom) to the source detector assembly. Unlike the simulation data in the previous two figures, all obstacles in these measurements were at 4 inch depths.

Whether these experimental data support the conclusion from the simulations that these particular objects should be detectable is, perhaps, better examined in an analysis of data obtained from a single, mock borehole having a pipe that either is or is not filled with water. Such analysis should remove most sources of systematic error. In other words, nothing differs in the two experiments except for the presence or absence of water in the pipe. Figure 10 presents the results of this analysis method. Due to the very high neutron-capture cross section of hydrogen and as observed in the simulations, one expects the number of detected photons within a broad energy range up to 2.223 MeV to generally increase when a pipe is filled with water. Increases of between 1 and 12% occurred in 3 out of 4 integrals of these difference spectra from 0 to 7 MeV; the parallel orientation of the steel pipe yielded a 0.4% decrease when filled with water. However, when limiting the integration range from 2.1 to 2.3 MeV, all 4 measurements yielded identical 3% increases in the number of photons in this narrow energy range. Additional analysis is needed to ascertain what other neutron-induced photons from other isotopes could be similarly focused on to aid/perform underground object detection based on a holistic analysis of the entire pulse-height spectrum.

Another expectation is that small errors in the detector energy calibrations will result in bipolar deviations in the difference spectra at energies of all spectral peaks. Narrow and relatively large peaks give rise to the most obvious effects of calibration offsets, but taking the difference of even broad continuum spectra gives erroneous results. Evidence of an energy-calibration issue at 0.5 MeV in the steel-pipe data is clear in Figures 9 and 10 and can also be discerned in the PVC-pipe data. However, a calibration offset across a broader energy range could explain some of the inconsistencies between the overall trends of these simulation and measurement results. Nevertheless, calibration drift during measurement operations is both expected and difficult to continuously avoid/correct, so any underground object detection system based on this neutron/photon method would be face this issue. Thus, while all four of these particular objects were detected, it will likely be very hard to maintain calibration sufficient to allow consistent performance.

Consequently, although some trends in these measured data are consistent with expectations from the simulations, object-orientation dependencies and calibration issues of the measurements prevent one from making decisive conclusions of what materials, in what environment, and using what data-analysis method would a specific object be detectable. As such, (1) some objects may go undetected and (2) when an object is detected, determining whether that object is benign clutter or an object of interest is unlikely.

Neutron/Neutron Method

Information about the materials surrounding a neutron source can be revealed by the photons that may be produced during neutron interactions with these materials or by the scattering neutrons themselves. The computer simulations discussed in the previous section simultaneously calculated the expected neutron detection rate for a ^3He neutron detector placed to one side of the lead shield, as shown in Figure 2. Figure 11 shows simulated neutron detection data for a ^{252}Cf neutron source probing the same test objects buried under 2 inches of sand. Although ^3He detectors are sensitive almost exclusively to

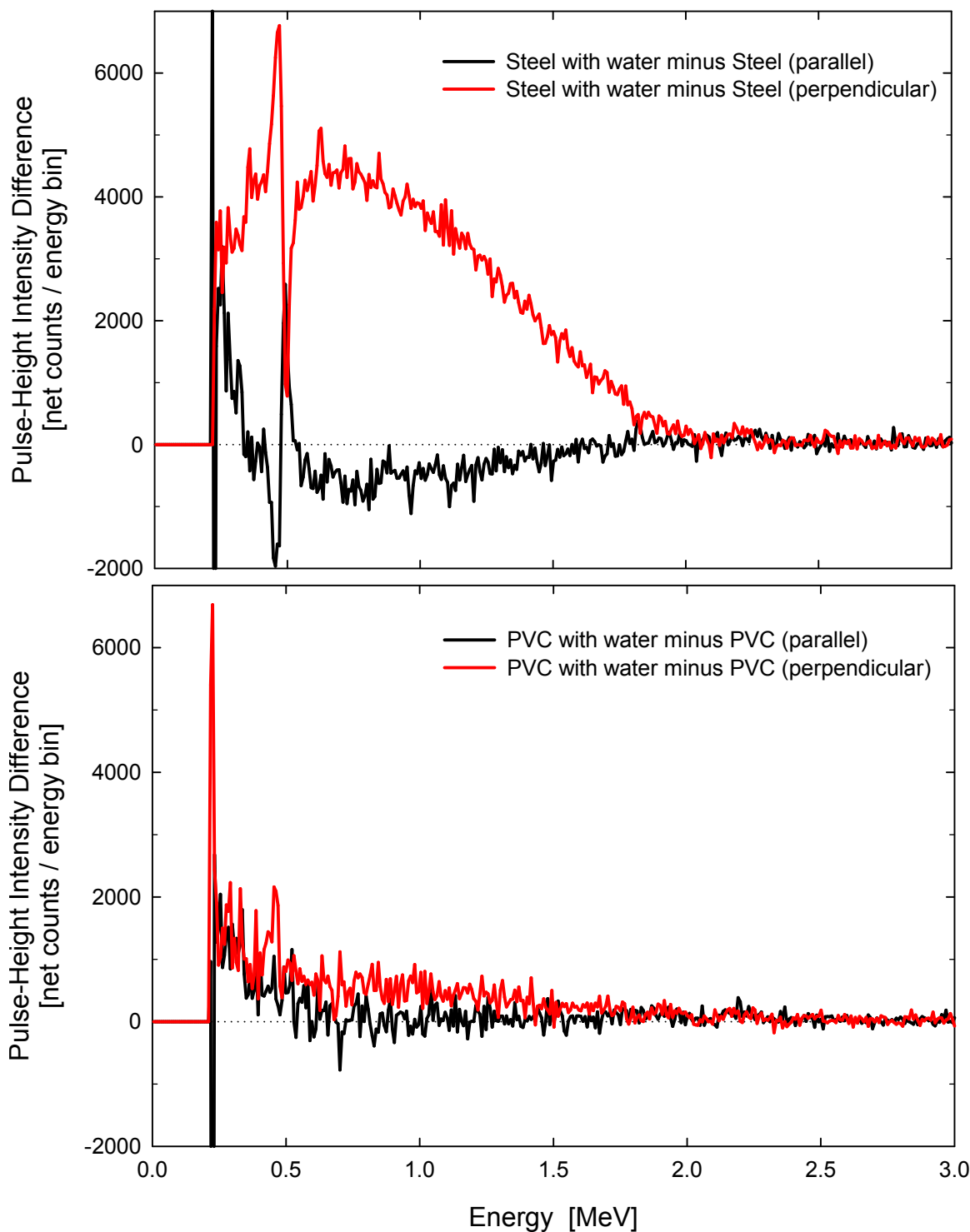


Fig. 10 Measured neutron/photon relative signal differences with and without water in a steel pipe (top) and PVC pipe (bottom) at 4 inch depths parallel and perpendicular to the source/detector assembly. The only change in each case is the addition of water in a pipe.

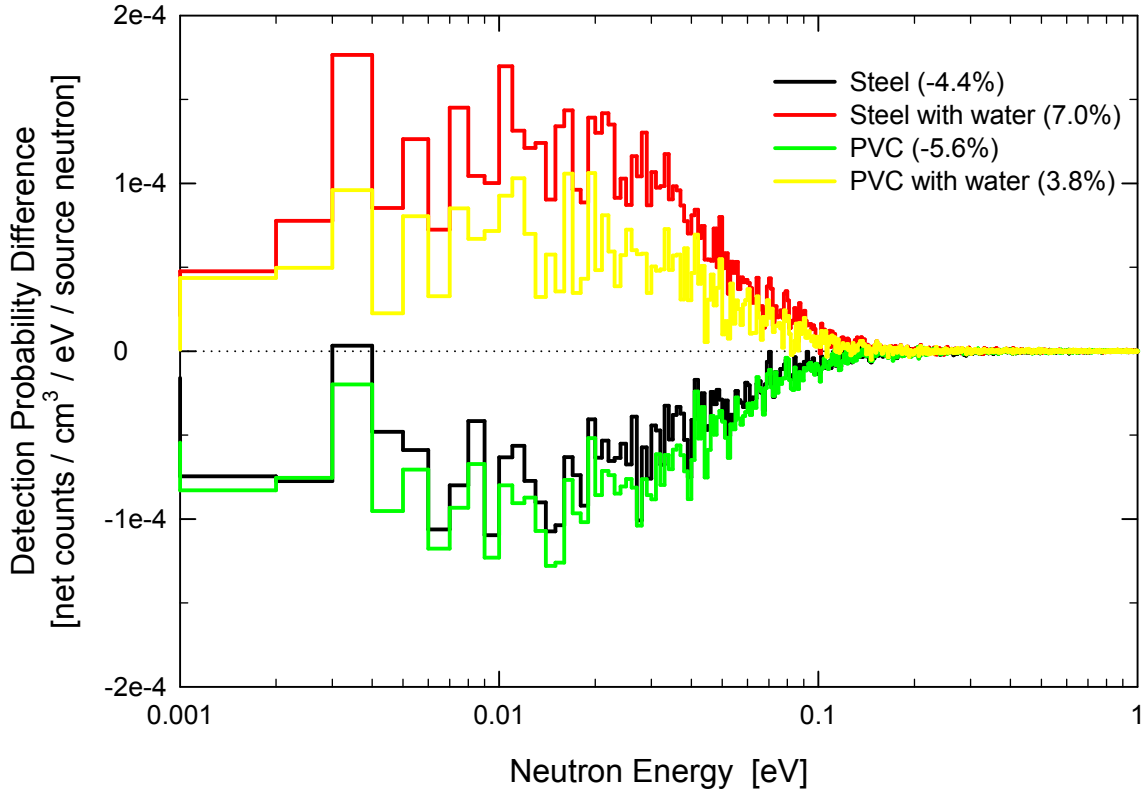


Fig. 11 Neutron/neutron simulation data plotted as signal differences with and without each pipe obstacle at 2 inch depths and parallel to the source/detector assembly. The relative differences shown in parentheses in the legend are for total numbers of detected neutrons.

thermal neutrons, these detectors simply count the number of all detected neutrons, regardless of their energy. However, in these simulations, the energy of a detected neutron can be and was recorded. The energy-dependent detection probability when an object is not present was subtracted from the probability when each object is present. Integrals over all energies were used to compute the percentage differences for each object relative to the case without an object present. The relative accuracy of the percentage differences P that are reported in the legend is (σ_P/P) ; ± 0.003 .

Similar trends are present in these data as are seen in the neutron/photon simulations shown previously in Figures 7 and 8 as well as in the photon/photon simulations in Figure 5. Empty pipes reduce the neutron detection rate by allowing the source neutrons to escape the vicinity of the detector. While the water in these pipes is a strong absorber of neutrons, which would otherwise reduce the neutron detection rate, water is also very effective at moderating (or thermalizing) neutrons, which increases the neutron detection rate by increasing the population of low-energy neutrons, which are much more likely to be detected by the ^3He detector used in these simulations. Predicting the outcome of these competing effects without a neutron transport simulation is difficult. (Note: although they were begun, no experimental measurements with a ^3He detector were completed due to resource constraints in this project.) It is seen clearly in these

simulation data that water's neutron-moderating properties dominate its neutron absorption properties.

These simulations show that by using a neutron source and detecting scattered neutrons, one could detect the presence of these particular objects. However, it should also be noted that some objects may have scattering effects that are balanced by absorption effects. For instance, an empty pipe that would normally reduce the neutron detection rate may be filled with just enough water to increase the neutron detection rate by a compensating amount, which would effectively make that object invisible to the neutron/neutron method of detection. Furthermore, unlike photon-based methods where spectroscopic data may be collected and analyzed to detect and characterize objects, the neutron/neutron method can only discern if an object or a variation in the native soil (i.e., clutter) is nearby based on a single parameter—neutron count rate. Thus, this method has more limited object detection and discrimination ability, which is almost entirely based on detecting changes in the concentration and distribution of hydrogen in the vicinity of the sensor.

Summary and Conclusions

The objective of this study was to determine the feasibility of using neutrons or gamma rays as a probe to ascertain the presence of underground objects forward of an underground boring tool. If this feasibility were established, a second objective was to determine how quickly and how far in front of the boring tool might the technique be useful. To assist in making these determinations, a series of calculations and experiments were performed for realistic, yet controlled, conditions. Underground objects common in urban locations were buried in trenches and ionizing radiation was used to detect the presence or absence of these objects. Some of the experiments clearly indicate the ability of ionizing radiation to detect the particular buried objects used in this study. Specifically, using a ^{252}Cf neutron source and either a gamma-ray spectrometer or a neutron counter to measure the return signal, was demonstrated to discern the presence of objects from a distance of 2 to 4 inches in soil. Likewise, interrogation with a ^{137}Cs gamma-ray source was similarly capable of detecting these objects in 2 inches of soil. All experimental results were corroborated by MCNP computer simulations.

However, characteristics of these detections also indicate that: (1) other objects may not be detected and (2) these methods are unlikely to be able to distinguish objects of interest from the clutter of natural variations and objects in the ground. A fundamental concern is that these experimental and simulated detections made use of a differential, or change, detection technique. Looking for a difference in the return signal when an object is present versus when that object is not present is only possible under artificial conditions. Additional research would be needed to determine and develop a method that is robust enough to be useful in field use. Without the option of differential measurements, the problem in the field will be recognizing objects of interest from “clutter”. Geologic media is heterogeneous, making it difficult to differentiate an object of interest from a background object, such as a rock. Nevertheless, SNL recommends that further research be pursued to clarify and expand upon this limited-scope effort.

Examination of the scientific and industrial literature indicated that there are other techniques under development that could be applicable. Pulsed fast-thermal neutron analysis, which uses microsecond pulses of 14 MeV neutrons from a deuterium-tritium

fusion source, is one technique that seemed promising but was not completely evaluated due to resource constraints. Another related technique of particular interest is associated-particle imaging (API). The developers of API contend that it is capable of imaging objects at a distance of several inches through soil or rock. Because current API systems are large, complex, and expensive, it was not possible to evaluate an API system during the project. However, after some false starts, SNL was able to contact a private company that is developing a capable API system, and made arrangements for this company to demonstrate their system to this project's Sponsor. Unfortunately, they were unable to fulfill their promise by the time of this report due to developmental problems encountered with their API system.

